


RESEARCH

Open Access



Upregulation of Beta4 subunit of BK_{Ca} channels in the anterior cingulate cortex contributes to mechanical allodynia associated anxiety-like behaviors

Huan Zhao^{1,2,4†}, Qian Xue^{1†}, Cong Li^{1,4,5†}, Qingchuan Wang^{1,6}, Shichao Han⁷, Yongsheng Zhou¹, Tao Yang¹, Yingli Xie¹, Hao Fu¹, Changbo Lu¹, Fancheng Meng¹, Ming Zhang¹, Yan Zhang⁴, Xianglong Wu⁶, Shengxi Wu¹, Min Zhuo^{2,3} and Hui Xu^{1,2*} 

Abstract

The anterior cingulate cortex (ACC) serves as a critical hub for the anxiety and pain perception. The large-conductance Ca²⁺-activated potassium channels, or BK_{Ca} channels, are ubiquitously expressed throughout the central nervous system including the cingulate cortex. However, what changes of cortical BK_{Ca} channels undergo in the ACC remains unknown in pain-related anxiety. In the present study, a significant upregulation of synaptic and non-synaptic BK_{Ca} channel accessory β4 subunits in the ACC was accompanied with pain-associated anxiety-like behaviors in the chronic compression of multiple dorsal root ganglia (mCCD) of the rat. NS1619, an opener of BK_{Ca} channels, significantly rescued the alteration of fAHP and AP duration of ACC pyramidal neurons in mCCD rats. The mRNA expression of BK_{Ca} β4 subunits was extremely upregulated in the ACC after mCCD with the increased amount of both synaptic and non-synaptic BK_{Ca} β4 subunit protein. Meanwhile, NS1619 reversed the enhanced AMPA receptor-mediated spontaneous excitatory postsynaptic current (sEPSC) frequency and the attenuated PPR of ACC neurons in mCCD rats. Local activation of BK_{Ca} channels in the ACC reversed mechanical allodynia and anxiety-like behaviors. These results suggest that the upregulation of postsynaptic and presynaptic BK_{Ca} β4 subunit may contribute to neuronal hyperexcitability and the enhanced synaptic transmission in the ACC in neuropathic pain state, and then may result in anxiety-like behavior induced by neuropathic pain.

Keywords: Anterior cingulate cortex, Anxiety, Large-conductance Ca²⁺-activated potassium channel, Excitability, Synaptic transmission

Introduction

Recent advances in our understanding of altered central nervous system activity in pain-related anxiety patients have emerged from human brain imaging. Although many brain sites including the prefrontal and the insular cortices have been implicated in the regulated network of both affective pain and anxiety, the anterior cingulate

cortex (ACC) serves as a critical hub for mood disorders, including anxiety and depression [1–4]. The stimulation of the ACC was sufficient to induce anxiety and depressive-like behaviors in naïve animals, while the ACC lesion prevented the pain anxiodepressive consequences of chronic pain without affecting the sensory mechanical allodynia [1]. Tons of evidence show that the ACC is involved in the pain-related negative affection [5]. However, the mechanisms underlying chronic pain related anxiety remain unclear in the ACC.

Clinical and experimental studies show that anxiety disorders and chronic pain often occur together. For example, anxious mood and other symptoms of anxiety were commonly seen in patients with chronic low back

* Correspondence: xubz@fmmu.edu.cn

[†]Huan Zhao, Qian Xue and Cong Li contributed equally to this work.

¹Department of Neurobiology and Collaborative Innovation Center for Brain Science, School of Basic Medicine, Fourth Military Medical University, Xi'an 710032, China

²Center for Neuron and Disease, Frontier Institute of Science and Technology, Xi'an Jiaotong University, Xi'an 710049, China

Full list of author information is available at the end of the article



pain, cancer pain and diabetic neuropathy as well. Anxiety and depressive disorders are two common psychiatric disorders in patients with breast cancer [6]. Chronic pain could induce anxiogenic effects in complete Freund's adjuvant (CFA) or neuropathic pain mice [7–9]. Greater pain intensity is correlated to more anxiety and depression in either spared nerve injury (SNI) mice or painful diabetic neuropathic patients [8, 10, 11]. A more recent study reported that cohabitation with a conspecific animal with chronic pain could potentially trigger anxiety in mice [12]. In turn, these negative emotional disorders aggravate pain perception. The patients with chronic back pain and pain-related anxiety are likely to have a tendency to overpredict pain events [13]. Previous studies also observed that anxiety might worsen pain perception [14–16]. The long-lasting anxiety exacerbated hypersensitive pain behaviors in the formalin rat model [17]. The interaction between chronic pain and anxiety is still not well understood.

BK_{Ca} channels are widely expressed throughout various tissues and cells in the central nervous system [18, 19], and play important roles in many physiological processes, including muscle contraction, circadian rhythm and hearing [20–22]. BK_{Ca} channels are tetramers characterized by a pore-forming α subunit containing seven transmembrane segments alone [23], or associated with accessory β subunits [20, 24]. Every β subunit has a specific tissue distribution and that it modifies channel kinetics as well as their pharmacological properties and the apparent Ca²⁺ sensitivity of the α subunit in different ways [23, 25–27]. Among the subunits of BK_{Ca} channels, α , β 2, β 4 types are predominantly expressed in central neurons [19]. The opening of BK_{Ca} channels allows rapid efflux of potassium ions, which effectively hyperpolarizes membrane potential, regulates membrane excitability [28, 29]. Recent work reported the downregulation and the decrease of BK_{Ca} channels in DRG and amygdala neurons in neuropathic pain and stress-induced anxiety [30–32], suggesting the possible functional involvement of BK_{Ca} channels in pain and anxiety. However, whether cortical BK_{Ca} channels undergo neuronal plastic changes in pain-related anxiety remains unclear. Our preliminary results showed a marked anxiety-like behavior in the newly established model of the chronic compression of multiple dorsal root ganglia (mCCD) [33]. Therefore, the aim of our present study was to investigate possible molecular mechanisms underlying pain-associated anxiety-like behaviors in the mCCD model at cortical level.

Materials and methods

Animals and mCCD model

All experiments were conducted on male Sprague-Dawley rats (weighing 150–200 g, 7–8 weeks old) purchased from the Laboratory Animal Center of Fourth Military Medical

University (FMMU), Xi'an, Shaanxi Province, China. All animals were housed under a 12 h dark–12 h light cycle with food and water provided ad libitum (temperature 22–26 °C, air humidity 40–60%). The rats were housed in our laboratory for at least 7 days before the initiation of the experiments. Rats were deeply anesthetized with an intraperitoneal (i.p.) injection of sodium pentobarbital (50 mg/kg body weight). All manipulations were done on the left side of the spinal column. Special care was paid to prevent infection and to minimize the influence of inflammation. The hair of the rats' lower back was shaved and the skin was sterilized with 0.5% iodine tincture. Sterile surgical instruments were used. With the rats in a prone position, an incision was made along the midline of the back at the L2 and L6 spinal level. Following separation of the paraspinal muscles from the transverse process, the L3–5 intervertebral foramina were exposed. L-shaped rods made of hollow stainless steel (4 mm in length and 0.5–0.8 mm in diameter) were carefully inserted into the L3, L4 and L5 foramina to compress the DRGs. All behavioral testing occurred between 09.00 and 12.00 h on the designated day of experiment. All experimental protocols were approved by the Institutional Animal Care and Use Committee of FMMU and animals were maintained and cared for in line with the guidelines set forth by the International Association for the Study of Pain.

Pain behavioral tests: mechanical allodynia

Paw withdrawal thresholds to mechanical stimulation were assessed as described [34] using Von-Frey filaments (Stoelting Corporation, USA). Animals were habituated to the behavioral test environment for 5–7 consecutive days before the testing. Mechanical allodynia was determined on ipsilateral and contralateral sides at postoperative 1, 3, 5, 7, 10 and 14 days. Animals were placed in plastic cages with a wire mesh floor. To test for the tactile threshold required to evoke withdrawal of the stimulated paw, von Frey filaments with different bending forces (2–15.0 g) were applied perpendicularly to the plantar part of the hindpaw in an ascending order. Each filament was applied 5 times to its minimum bending force, and a paw withdrawal threshold was defined as three positive responses. To avoid potential tissue damage, the cut-off threshold was assigned as 15.0 g-force.

Rotator rod

Functional motor impairment was evaluated by the accelerating rotator rod test. A 5-min activity test was performed for each rat. Subjects received 5 consecutive training trials on the rotate rod, as previously described [35]. The rod accelerated from 4 rpm to 40 rpm over a 5-min period, and the latency (in seconds) for the animal to fall off the drum was recorded. The rotator rod is covered with fine grit sandpaper to provide a uniform

surface and to reduce slipping [36]. The rotate rod was interfaced to a computer that collected the time each subject remained on the rod up to a maximum time of 360 s. After the 5 training trials were complete, averages of the last 3 trials were calculated and animals which failed to meet a criterion of 7 s were given additional training trials until their final 3 training trials averaged 7 s. The rats were trained on the rotarod for three consecutive days. The motor activity on the rotate rod was testing on postoperative day 7, and the mean latency for the animal to fall off the drum in the three test trials was recorded.

Elevated plus maze

The elevated plus maze was a cross-shaped platform positioned 80 cm above the floor with two open arms (50.17 cm × 10.8 cm) and two closed arms (50.17 cm × 10.8 cm × 40.01 cm) on opposing sides of a central square platform (10.8 cm × 10.8 cm). It is a well-established rodent test used to characterize anxiety-like behaviors. Rats were allowed to habituate to the testing room for 2 days before the test, and were pre-treated with gentle handling two times per day to eliminate their nervousness. For each test, individual animals were placed on the centre square, facing an open arm, and allowed to move freely for 5 min. Mice were videotaped using a camera fixed above the maze and analyzed with a video-tracking system. The number of entries and time spent on each arm were recorded. The elevated plus maze was cleaned by 70% ethanol after each rat to remove any possible olfactory cues.

Open field Test

The open field apparatus recorded as a measurement for locomotor activities was a black square box (90 cm × 90 cm × 60 cm). At the start of the test, each rat was placed at the centre of the box and allowed to explore the field freely for 15 min, during which its behavior was recorded by a video camera mounted above the maze. The field was divided into nine equal segments in the analyzed system. Anxiety-like behavior was determined by measuring the percentage of time spent in the center of the open field. The field was cleaned by 70% ethanol to remove any possible olfactory cues between each animal. An experimenter blind to treatment groups handled the animals and analyzed the video recordings.

Quantitative (QT) real-time RT-PCR

mRNA expression of α and β (1–4) subunits of BK_{Ca} channels was evaluated by reverse transcription PCR. Total RNA was extracted from the ACC and the insular cortex and purified using RNAiso Plus and a Total RNA Isolation Kit (Takara, Otsu, Shiga, Japan).

The OD260/280 ratio of the RNA samples was measured, and the samples with a ratio of 1.8–2.0 were used for reverse transcription. In total, 0.5 mg RNA was reverse-transcribed to cDNA by using Prime Script™ RT Reagent Kit (Takara). The reactions were performed at 37 °C for 15 min and then 85 °C for 5 s. Quantitative RT-PCR analyses were performed in triplicate by using SYBR® Premix Ex Taq™ Kit (TaKaRa) and detected by using a Bio-Rad iQ5 Multicolor Real-Time PCR Detection System (Bio-Rad, Hercules, CA, USA). The data were normalised to β -actin, and the comparative cycle threshold (Ct) method ($2^{-\Delta\Delta Ct}$) was used to calculate the relative quantity of target mRNAs.

Primers were designed by using the software Primer-BLAST developed at the National Center for Biotechnology Information (NCBI, Bethesda, MD, USA) and based on the software Primer 6. To check any possible genomic contamination of cDNA samples, each couple of primers was separated by at least one intron (minimum size of 1000 base pair) on the corresponding genomic DNA. The primer sequences were listed in Table 1.

The following thermal cycle condition was employed to reverse-transcribe the mRNA: an initial denaturation at 95 °C for 30 s, followed by 40 cycles of denaturation at 95 °C for 5 s, and annealing at 60 °C for 30 s were performed.

Western blot analysis

Western blot analysis was performed as described previously [32]. Tissue samples from the bilateral ACC were dissected from the brain slices under the anatomical microscope. 30 μ g of total proteins were separated by electrophoresis on SDS-PAGE and then transferred to a polyvinylidene difluoride membrane (Invitrogen). The synaptosome was digested to yield an insoluble PSD-enriched (synaptic) membrane fraction and a soluble non-PSD enriched (peri/extrasynaptic and presynaptic) membrane fraction [37–39]. A clear separation of PSD and non-PSD membranes was collected as our previous study [39].

Membranes were incubated with primary antibody against BK_{Ca} α subunits (1:400, Alomone Labs, Jerusalem, Israel; product no., APC-021), BK_{Ca} β 4 subunit (1:200, Alomone Labs, Jerusalem, Israel; product no., APC-061) or β -actin (1:1000, Sigma) as loading control overnight at 4 °C. Then the membranes were incubated with horseradish peroxidase-conjugated secondary antibodies (anti-rabbit IgG) for 1 h at 37 °C. The density of each protein band on the membrane was scanned using a FluroChem FC system (Alpha Innotech, San Jose, California, USA) and is presented as a densitometric ratio between the protein of interest and the loading control.

Table 1 Sequence of primers used for RT-PCR

Gene	Accession no.	Sequence of; F, forward primer; R, reverse primer	Region	Product
β -actin	Rat NM-031144	F: 5'-ATGGTGGGTATGGGTCAGAAGG-3' R: 5'-TGGCTGGGGTGTGAAGGTC-3'	208–472	265 bp
BK_{Ca} α subunit	Rat NM-031828.1	F: 5'-CAGCACTCCGACACTA-3' R: 5'-ATCACCATAACAACCACCATCC-3'	3774–3879	106 bp
BK_{Ca} $\beta 1$ subunit	Rat 019273.1	F: 5'-CGCCATCACTTACTACATCCT-3' R: 5'-GACCTTCTTCACATCAACCAA-3'	394–682	289 bp
BK_{Ca} $\beta 2$ subunit	Rat 176,861.1	F: 5'-CGGACCTTTCATCTTACAGAC-3' R: 5'-CAGCAGTGTGATCCAGTAG-3'	22–210	189 bp
BK_{Ca} $\beta 3$ subunit	Rat 001104560.2	F: 5'-CGCTCTGATTGTTGGTTGGT-3' R: 5'-CTCTGTTCTTCCCTGACTCTT-3'	899–1059	161 bp
BK_{Ca} $\beta 4$ subunit	Rat 023960.2	F: 5'-CATCTGTGCTCTTCATCTTC-3' R: 5'-TGGTGCTGGTCGCTGTGTA-3'	102–335	234 bp

RT-PCR real-time polymerase chain reaction, BK_{Ca} large-conductance, calcium-activated potassium

Whole-cell patch-clamp recording

The animals were killed by being rendered unconscious by 4% isoflurane in air and then killed by cervical dislocation. Brain slices (300 μ M) containing the ACC were cut at 4 °C with a vibratome in oxygenated artificial CSF containing (in mM): 124 NaCl, 2.5 KCl, 25 NaHCO₃, 2 CaCl₂, 2 MgSO₄, 1 NaH₂PO₄, and 20 D-glucose, pH 7.4. For electrophysiology, brain slices were transferred to a submerged recovery chamber with oxygenated ACSF at room temperature. After 1 h of the recovery, slices were placed in a recording chamber on the stage of an Olympus microscope with infrared digital interference contrast optics for visualization of whole-cell patch-clamp recordings. The recording pipettes (3–5 M Ω) were filled with a solution containing (in mM) 145 K-gluconate, 5 NaCl, 1 MgCl₂, 0.2 EGTA, 10 HEPES, 2 Mg-ATP, 0.1 Na₃-GTP, and 10 phosphocreatine disodium (adjusted to pH 7.2 with KOH). For firing rate recording, interneurons and pyramidal neurons were identified by their different firing patterns and morphology. The typical firing pattern of pyramidal neurons showed significant firing frequency adaptation, whereas interneurons showed fast-spiking APs followed by pronounced hyperpolarization, lower rheobase current and higher input resistance [40]. In the present study, layer II/III pyramidal neurons in the ACC were recorded. Access resistance 15–30 M Ω was considered acceptable. Data were discarded if access resistance changed > 15% during an experiment. Data were filtered at 1 kHz, and digitized at 10 kHz.

Passive membrane properties

Off-line analysis was performed using Clampfit version 10.4 (Axon Instruments). Resting membrane potential (RMP) was the low-pass readout of the electrode amplifier and was not corrected for liquid junction potential (~ 12 mV) after terminating the recording. The membrane

potential was measured immediately after establishing the whole cell configuration. Only neurons that had a resting membrane potential more negative than – 60 mV were further investigated.

Active membrane properties and firing patterns

Action potentials (APs) were detected in response to suprathreshold current injections from a holding potential around – 60 mV. Depolarizing currents of – 100~480 pA (500ms duration) were delivered in increments of 20 pA until an AP was evoked. The rheobase was defined as the minimum current required to evoke an action potential. The AP voltage threshold ($V_{\text{threshold}}$) was defined as the first point on the rising phase of the spike at which the change in voltage exceeded 50 mV/ms. The spike amplitude was quantified as the difference between the $V_{\text{threshold}}$ and the peak voltage. The duration of the AP was measured at the threshold voltage. The spike width was measured at 1/2 of the total spike amplitude (measured from the $V_{\text{threshold}}$ level). The time to the peak of fast component of the after hyperpolarization (fAHP) was estimated as the time from the peak of the action potential to the most negative voltage reached during the fAHP (defined as the peak of fAHP). The amplitude of fAHP was estimated as the difference between the $V_{\text{threshold}}$ and the peak of fAHP. The waveform characteristics of the action potentials recorded from neurons of sham and mCCD rats, i.e., rise time, rise slope, decay time and decay slope, were determined using Clampfit10.4 software (Axon Instruments). The properties of firing patterns and hyperpolarizing responses were analyzed from voltage response to injected current pulses.

In BK_{Ca} current experiments, TTX (1 μ M), apamin (200 nM) and 4-AP (10 mM) were routinely added to extracellular solutions to block action potentials and

minimize contamination by small-conductance, calcium-activated K^+ (SK) currents [41] and voltage-dependent K^+ (K_V) currents, respectively [42, 43]. In voltage-clamp mode, macroscopic outward currents were elicited from a holding potential of -60 mV, stepping to $+40$ mV for 400 ms in 10 mV increments. BK_{Ca} currents were isolated by application of paxilline ($10 \mu\text{M}$), an antagonist of BK_{Ca} channels [44, 45], by subtracting currents in the presence of paxilline from the initial current.

ACC cannulation and microinjection

Rats were anesthetized by intraperitoneal injections of sodium pentobarbital (40mg / kg). Rat heads were secured on a stereotaxic frame, and 24 gauge guide cannulae were implanted bilaterally into the ACC (0.5 mm anterior to bregma, ± 0.4 mm lateral from the midline, 2.5 mm beneath the surface of the skull). The rats were given 1 week to recover after the cannula implantation. The 30 gauge injection cannula used was 0.1 mm lower than the guide cannula. For the microinjection, the animals were placed individually in an induction chamber, and anaesthesia was induced with 2.5% isoflurane (RWD, Shenzhen, China) in 100% oxygen with a delivery rate of 0.5 l/min until loss of righting reflex. Anaesthesia was then maintained with 1.5% isoflurane in 100% oxygen with a flow of 0.5 l/min delivered by a face mask. The selective BK_{Ca} channel agonist NS1619 ($10 \mu\text{M}$, $0.5 \mu\text{l}$) (Tocris) was infused into each side of the ACC at a rate of $0.5 \mu\text{l}/\text{min}$; an equivalent volume of ACSF ($0.5 \mu\text{l}$) was used as a control using a syringe driven by an infusion pump (RWD, Shenzhen, China). After infusion, the cannula was left in place for an additional 2 min to allow the solution to diffuse away from the cannula tip. The injection sites were confirmed at the end of all experiments, and sites outside of the ACC region were excluded from the study. Elevated plus maze, open field tests and mechanical threshold were then reassessed 30 min after the microinjection of either ACSF or NS1619 in the ACC within 7–10 days after the compression of multiple DRG.

Chemicals

(1,3-dihydro-1-[2-hydroxy-5-(trifluoromethyl)-phenyl]-5-(trifluoromethyl)-2H-benzimidazol-2-one), NS1619 (Tocris), a specific BK_{Ca} channel opener; Paxilline (alomo), a BK_{Ca} channel blocker; NS1619 and paxilline were both dissolved in dimethylsulfoxide (DMSO), and then diluted in ACSF to the final concentration of $10 \mu\text{M}$.

Statistical analysis

Statistical analyses were performed by using SigmaStat 3.5 and GraphPad Prism 6 softwares. All data sets were tested for normality for t-test, and if normality test (Shapiro–Wilk) failed, Mann–Whitney Rank Sum test was used.

Results are expressed as mean \pm s.e.m. $p < 0.05$ is considered as a significant change. The two-way repeated-measure analysis of variance (ANOVA) was used to compare the differences between groups in the pain behavior testing and to analyze BK currents in sham and mCCD groups.

Results

Enhanced anxiety-like behaviors in mCCD rats

To explore the pain-associated anxiety in mCCD rats, the rats were subjected to elevated plus maze (EPM) and open field tests on postoperative day 7–14. In the elevated plus maze, the increase of the time spent in the open arms is interpreted as a measure of decreased anxiety-like behaviors. The mCCD rat exhibited significantly lower entries and less time in the open arms than sham rats (Fig. 1a). The mCCD rat spent less time in the center of the open field (Fig. 1b), which is interpreted as anxiety-like behaviors [46]. Because the open field test can also be used as a measure of overall activity, we measured the total distance traveled in the open field. There was no difference in the total distance between mCCD and sham rats (Fig. 1b). The mechanical pain threshold was examined on days 1, 3, 5, 7, 10 and 14, postoperatively, in mCCD and sham rats. This increase in mechanical sensitivity was reflected in the large bilateral decrease in the hind paw withdrawal thresholds (defined as the minimum bending force required to elicit 50% response incidence) after mCCD. Peak of mechanical hypersensitivity occurred between 7 and 14 d after mCCD (Fig. 1c). However, neither the time spent on accelerating rotator rod nor the total distance travelled in the open field tests changed compared with those of sham group (Fig. 1d and b), showing that there was no difference in locomotor activity between mCCD and sham groups. These data demonstrate that neuropathic pain enhances anxiety-like behaviors in mCCD rats.

Elevated excitability of ACC pyramidal neurons in mCCD rats (Table 2)

To investigate whether the intrinsic properties of ACC pyramidal neurons are altered after mCCD, we studied the firing patterns and the action potential in pyramidal neurons in the layer II or layer III of acutely isolated the ACC slices from mCCD or sham rats. Whole-cell patch clamp recordings were performed on ACC pyramidal neurons on postoperative 7–14 days after mCCD, a time when the maximal behavioral sensitization can be observed. Recorded neurons were identified as pyramidal neurons based on their ability to show spike frequency adaptation in response to prolonged depolarizing-current injection [39]. We compared the passive membrane and the first action potential properties in a train elicited by a 300 pA, 500 ms depolarizing current (Fig. 2a). There were no

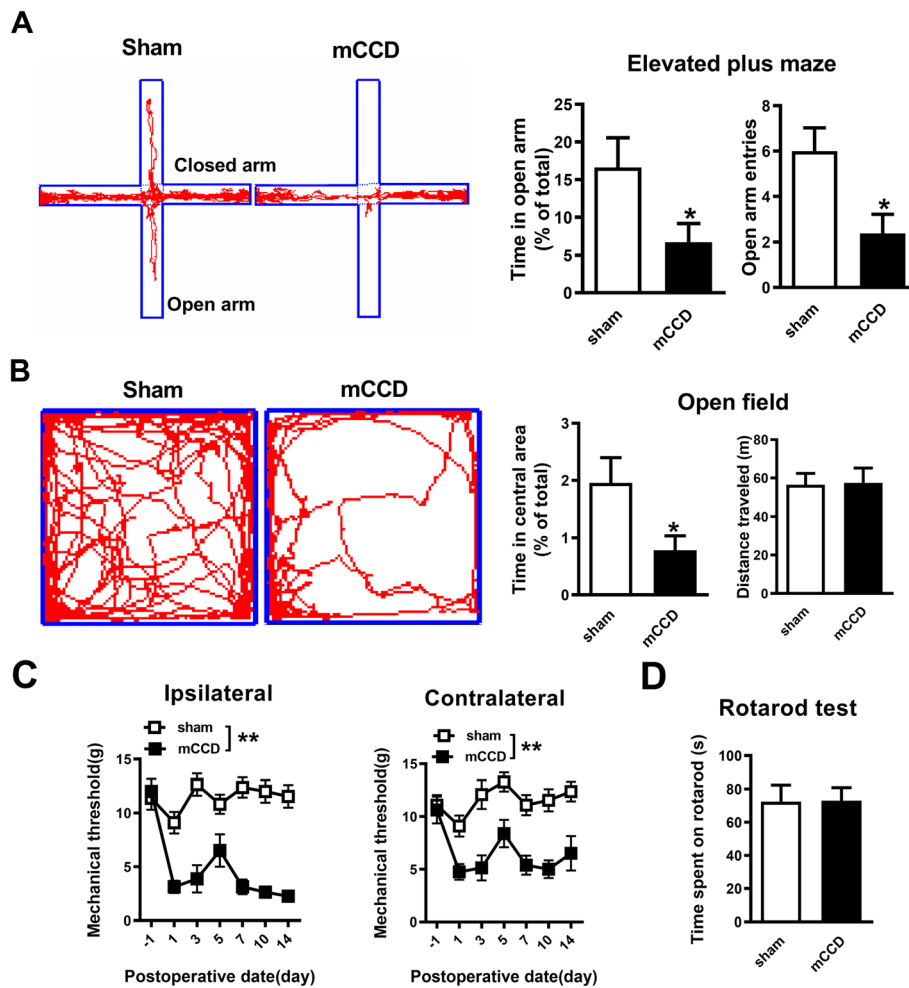


Fig. 1 Enhanced anxiety in neuropathic pain rats following mCCD. **a**, Representative traces show the movement of sham and mCCD rats in elevated plus maze for 5 mins, mCCD rats ($n = 13$) spent less time in the open arms of elevated plus maze and showed a decrease in open arm entries compared with sham rats ($n = 13$). **b**, Representative traces show the movement of sham and mCCD rats in the open field test over a period of 15 min, mCCD rats ($n = 13$) spent significantly less time in the central zone in the open field test compared with sham rats ($n = 13$). Total distance travelled in the open field test was not changed compared with sham rats. **c**, The time course of ipsilateral and contralateral hind paw mechanical withdrawal thresholds after mCCD (sham group: $n = 11$, mCCD group: $n = 8$). The ipsilateral and contralateral hind paw withdrawal thresholds were significantly decreased below baseline on the 1st postoperative day and reached their lowest peak during the 7th to 14th postoperative day. **d**, Motor performances on the accelerating rotarod of mCCD rats (mCCD: $n = 7$, sham: $n = 7$). $*p < 0.05$, $**p < 0.01$ compared with that of sham group

Table 2 Intrinsic passive and active properties of ACC pyramidal neurons after mCCD

	sham	mCCD
Resting membrane potential (mV)	-65.32 ± 1.26 ($n = 38$)	-64.79 ± 0.76 ($n = 49$)
R_m (m Ω)	75.08 ± 4.01 ($n = 35$)	104.5 ± 10.15 ($n = 29$)*
C_m (pF)	138.4 ± 12.38 ($n = 35$)	168.9 ± 14.21 ($n = 29$)
Rheobase (pA)	129.4 ± 10.66 ($n = 34$)	99.57 ± 5.91 ($n = 47$)*
Action potential threshold (mV)	-31.47 ± 1.29 ($n = 34$)	-30.02 ± 0.94 ($n = 47$)
Action potential amplitude (mV)	96.05 ± 2.17 ($n = 32$)	88.82 ± 2.07 ($n = 47$)*

* $p < 0.05$, compared with that of sham group

significant differences in parameters, such as RMP, membrane capacitance (C_m), action potential threshold among ACC neurons between sham and mCCD rats. However, the membrane resistance (R_m), rheobase, action potential amplitude, fAHP peak voltage, duration, half width, decay time, decay slope, rise time and rise slope were significantly changed (Fig. 2 and Table 2). R_m was larger ($p < 0.05$), rheobase was smaller ($p < 0.05$), action potential amplitude was smaller ($p < 0.05$), the fAHP for the first three APs in a train was reduced (Fig. 2c), duration and half-width was significantly increased (Fig. 2d and e), decay time and rise time was longer (Fig. 2f and i), and decay slope and rise slope was slower (Fig. 2g and h) in ACC pyramidal neurons of mCCD rats.

Effects of NS1619 and paxilline on the excitability of pyramidal neurons in the ACC following mCCD

To test whether the role of BK_{Ca} channels in the parameters' variation of ACC pyramidal neurons in mCCD rats, action potentials were generated in ACC pyramidal neurons in the presence or absence of NS1619 ($10 \mu M$). As illustrated in Fig. 3, in mCCD rats, NS1619 significantly increased the peak of fAHP for the first three action potentials in the train elicited by 300 pA, decreased the duration and half-width and increased the decay time. While paxilline ($10 \mu M$), a blocker of BK_{Ca} channel, failed to affect those parameters in the sham rats. The results implicate the functional roles of BK_{Ca} channel in the control of intrinsic excitability in ACC pyramidal neurons after neuropathic pain.

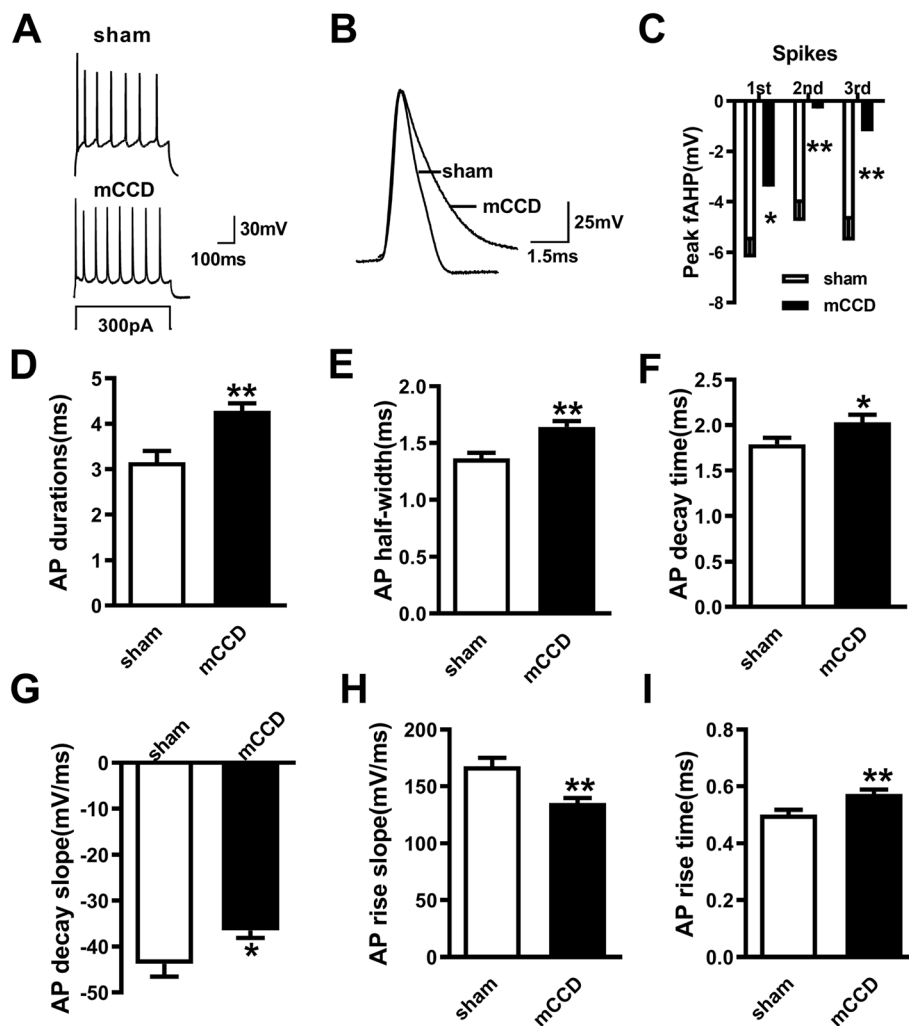


Fig. 2 Elevated excitability of pyramidal neurons in the ACC in mCCD rats. **a**, Representative traces showing the firing property in the neurons from ACC of sham and mCCD rats response to a 300 pA depolarizing current injection (500 ms). **b**, Representative recording of the first spike in the neurons from sham and mCCD slices. **c**, The amplitude of fAHP of the first three spikes in a train. **d-i**, The duration (**d**), half width (**e**), decay time (**f**), decay slope (**g**), rise slope (**h**), rise time (**i**) of the first spike of pyramidal neurons from mCCD and sham rats (mCCD: $n = 24$; sham: $n = 35$) * $p < 0.05$, ** $p < 0.01$ compared with that of sham group

Reduced BK_{Ca} currents of ACC neurons in mCCD rats

To test BK_{Ca} current of ACC pyramidal neurons in mCCD rats, we performed voltage-clamp recordings. Paxilline (a selective antagonist of BK_{Ca} channel) is often used to confirm the BK current. The membrane potential of recorded neurons was stepped from a holding potential of -60 mV to +40 mV in 10 mV increments. We first identified the recorded neurons as pyramidal neurons based on their ability to show spike frequency adaptation in response to 500 ms

depolarizing-current injection. The spikes were eliminated by adding the TTX (1 μM), apamin (200 nM) and 4-AP (10 mM) to ACSF to block action potentials, and minimize contamination by small-conductance, calcium-activated K⁺ (SK) and voltage-dependent K⁺ (KV) currents, and then switched to perfusate containing TTX, apamin, 4-AP and paxilline (10 μM) (+TTX + apamin + 4-AP + Paxilline, wash-in duration: 5 min) to obtain paxilline-sensitive current by subtracting +TTX + apamin + 4-AP + Paxilline currents

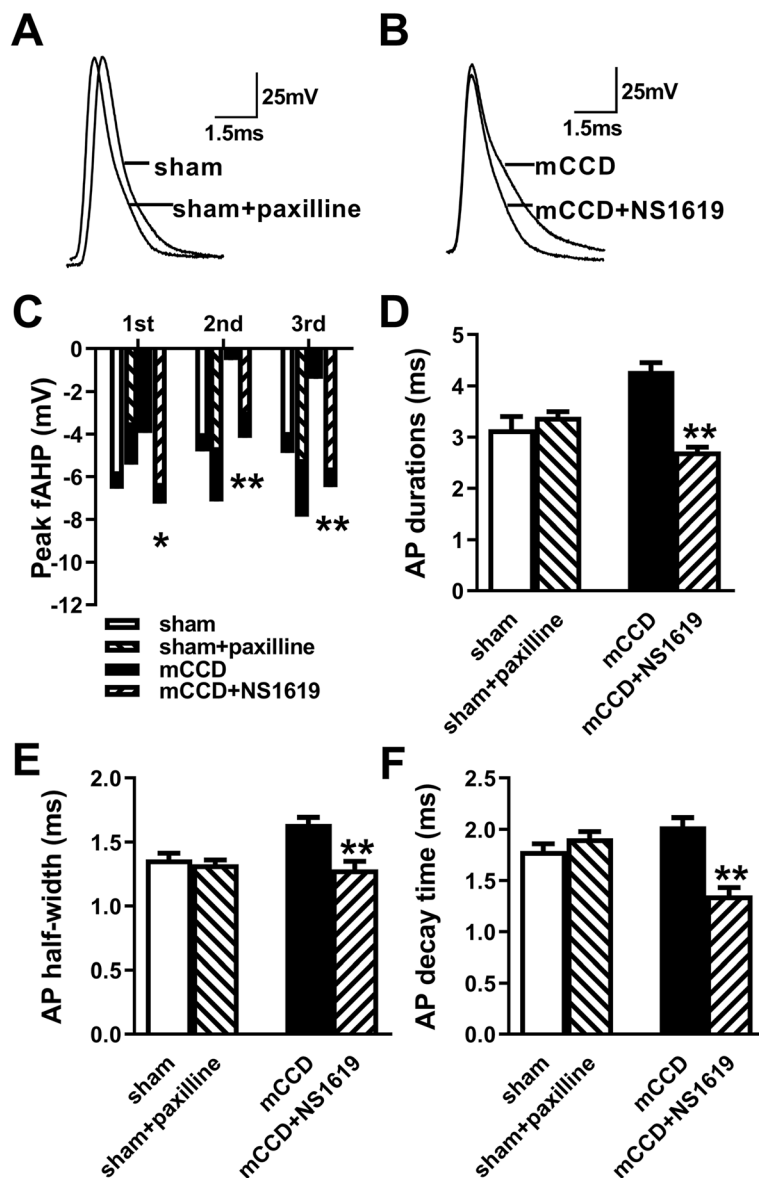
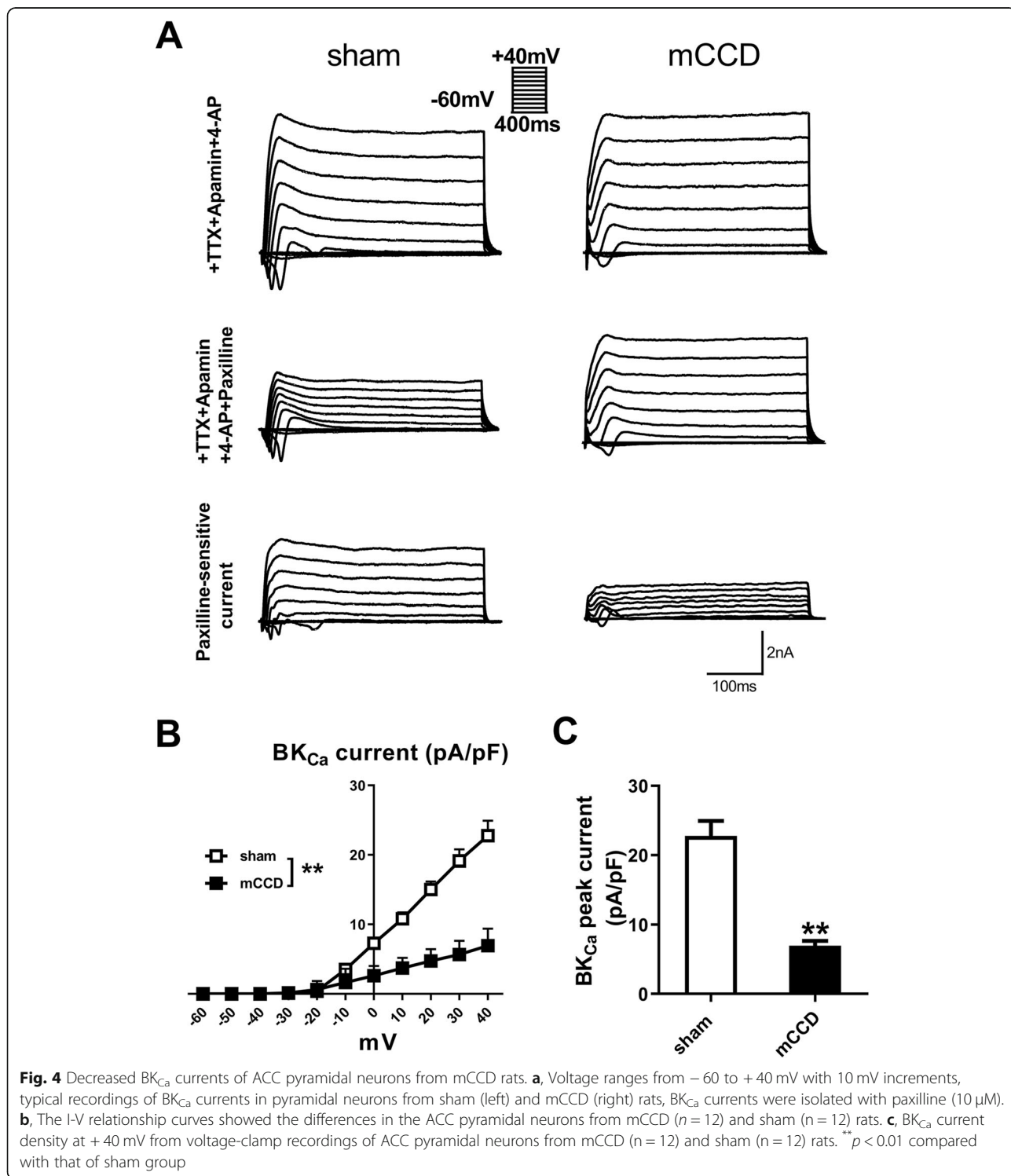


Fig. 3 Effects of NS1619 and paxilline on the excitability of pyramidal neurons in the ACC following mCCD. **a-b**, Representative recording traces of the first spike in the neurons from sham and mCCD slices in the presence of paxilline or NS1619 respectively. **c**, Histograms show the amplitude of fAHP of the first three spikes from the sham group in the absence and presence of paxilline (10 μM) (sham, *n* = 30, sham+paxilline: *n* = 10), and from the mCCD group in the absence and presence of NS1619 (10 μM) (mCCD: *n* = 48, mCCD+NS1619: *n* = 17). **d-f**, Histograms show AP duration (**d**), AP half-width (**e**) and AP decay time (**f**) from the sham group in the absence and presence of paxilline (sham: *n* = 30, sham+paxilline: *n* = 10), and from the mCCD group in the absence and presence of NS1619 (mCCD: *n* = 48, mCCD+NS1619: *n* = 17). **p* < 0.05, ***p* < 0.01 compared with that of mCCD group

from +TTX + apamin+ 4-AP currents. Paxilline-sensitive BK_{Ca} currents were significantly reduced in the mCCD rats compared with those of sham rats (Fig. 4a and b). I-V curve analysis also showed that BK_{Ca} currents were strongly decreased after mCCD

(Fig. 4b). The amplitude of currents at the membrane potential of +40 mV in the mCCD group was significantly reduced compared with that of sham group (Fig. 4c). In page 10, line 36, authors should use same style of °C.

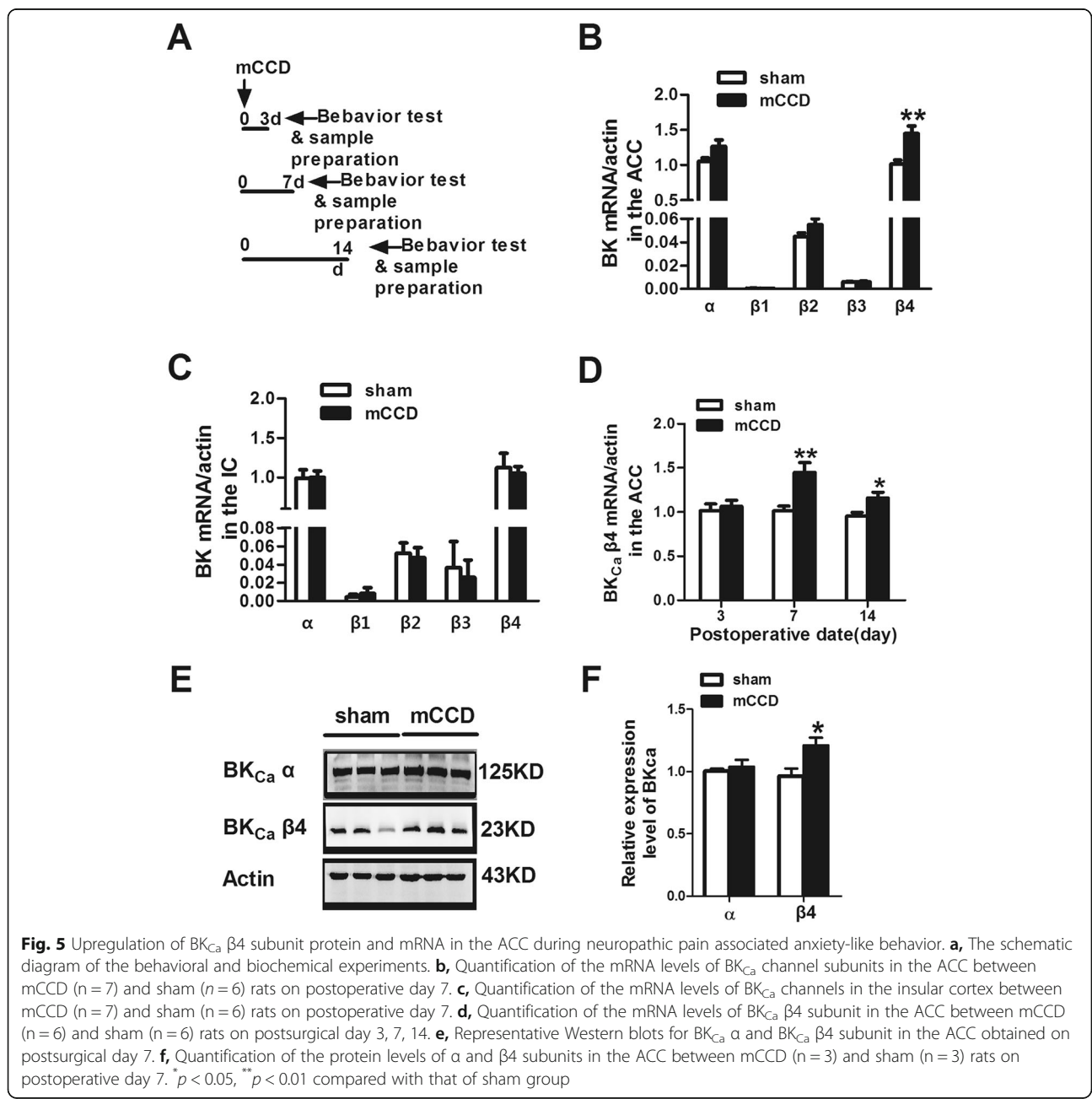


Up-regulation of BK_{Ca} β4 subunit in the ACC in neuropathic pain

To investigate whether the expression of BK_{Ca} channels is involved in the ACC in neuropathic pain state, we performed RT-PCR and Western blotting to examine the mRNA and protein levels of BK_{Ca} channels (Fig. 5). Our results showed that there were expressed in mRNA level of BK_{Ca} channels in the ACC and the insular cortex on day 7 after the surgery, including α subunit, the dominant subunit of BK_{Ca} channels, and β1–4 subunits (Fig. 5b and c). mRNA expression of BK_{Ca} β4 subunit was remarkably increased in the ACC on postsurgical day 7 (Fig. 5d), while

there were no differences in mRNA level of α subunit, the dominant subunit of BK_{Ca} channels, and β1–3 subunits (Fig. 5b) in the ACC on day 7 after surgery. To further test whether the change of BK_{Ca} β4 subunit is region specific for the ACC after neuropathic pain, we also tested the mRNA levels of BK_{Ca} subunits in the insular cortex, another brain region important for pain-related perception. In contrast, no difference of the expression of all subunits of BK_{Ca} channels in the insular cortex was observed on postsurgical days 7 (Fig. 5c).

Moreover, we examined the abundance of BK_{Ca} β4 subunit in the ACC in different times on day 3, 7, 14 after



surgery (Fig. 5d). Our results showed that the abundance of BK_{Ca} β4 subunit was significantly increased on postsurgical day 7 and 14, but not on day 3. Similarly, the protein expression of BK_{Ca} β4 subunit in the ACC from mCCD rats was also increased on postsurgical day 7 compared with sham rats (Fig. 5e and f). All these results indicate that the expression of BK_{Ca} β4 subunit is specifically increased in the ACC during neuropathic pain.

To determine whether postsynaptic or presynaptic BK_{Ca} subunits are involved in neuropathic pain in mCCD rat, we investigated the abundance of BK_{Ca} α and β4 subunits in different subcellular fractions of the ACC on day 14 after surgery (Fig. 6). Our results showed that BK_{Ca} β4 subunit was located at both the extra-synaptic and pre-synaptic non-PSD, and the synaptic PSD membrane

fractions in the ACC, while BK_{Ca} α subunit only predominated at the synaptic PSD membrane fraction in the ACC of sham rats (Fig. 6). We found that the abundance of non-PSD and synaptic PSD BK_{Ca} β4 were significantly increased in the ACC on postsurgical day 14 following mCCD (Fig. 6, non-PSD fraction: sham group, 100 ± 12%, n = 6, mCCD group, 224 ± 32%, n = 6, *p < 0.05; PSD fraction: sham group, 100 ± 32%, n = 6, mCCD group, 164 ± 37%, n = 6, *p < 0.05). Moreover, BK_{Ca} α subunit was no significantly changed in the PSD fraction in the ACC of mCCD rats on postoperative day 14 (Fig. 6, sham group, 100 ± 17%, n = 6, mCCD group, 91.4 ± 14%, n = 6, p > 0.05). Together, these data suggest that the synaptic and presynaptic BK_{Ca} β4 subunit might be increased in the ACC during neuropathic pain.

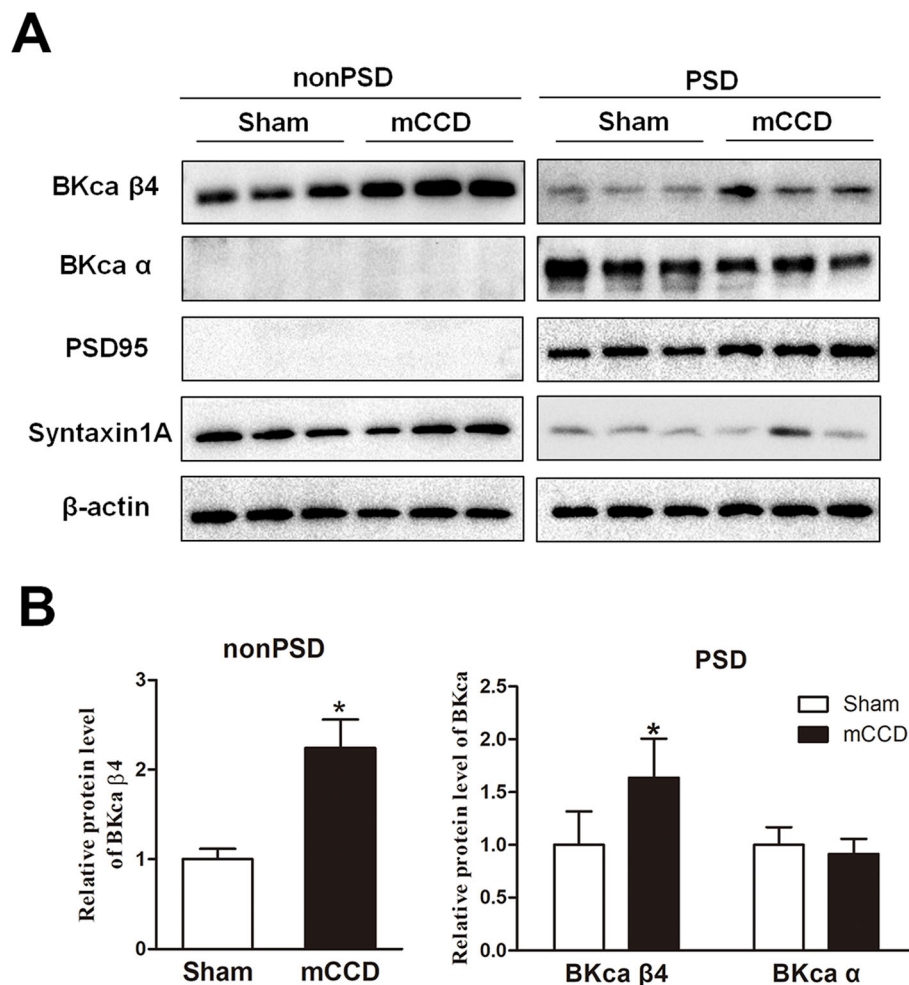


Fig. 6 Postsynaptic and presynaptic upregulation of BK_{Ca} β4 subunit protein in the ACC during neuropathic pain associated anxiety-like behavior. **a**, Representative Western blots for PSD 95, syntaxin 1A, BK_{Ca} β4 and BK_{Ca} α subunits in the non-PSD and PSD membrane fractions of the ACC in sham and mCCD rats on postoperative day 14; **b**, BK_{Ca} β4 subunit was significantly enhanced in the PSD and non-PSD fractions of the ACC from mCCD (PSD fraction: 164 ± 37%, n = 6, *p < 0.05; non-PSD fraction: 224 ± 32%, n = 6, *p < 0.05) rats on postoperative day 14 compared with those in sham rats (PSD fraction: 100 ± 32%, n = 6; non-PSD fraction: 100 ± 12%, n = 6). BK_{Ca} α subunit showed no significant change in the PSD fraction between sham (100 ± 17%, n = 6) and mCCD (91.4 ± 14%, n = 6, p > 0.05) rats on postoperative day 14

NS1619 reversed the enhanced AMPA receptor-mediated sEPSC frequency of ACC neurons in mCCD rats

BK_{Ca} channels have been proposed to limit calcium entry and transmitter release by reducing the duration of the pre-synaptic spike at neurosecretory nerve terminals [47]. It is possible that loss of function of BK_{Ca} channels may lead to the enhancement of basal excitatory synaptic transmission. To explore whether there is any change in the basal excitatory synaptic transmission in the ACC during neuropathic pain, we recorded AMPAR-mediated sEPSCs in pyramidal neurons in the layer II or layer III of acutely isolated ACC slices from mCCD or sham rats on postsurgical day 7 in

the presence of AP-5 (50 μM) and picrotoxin (100 μM) (Fig. 7). We found that the sEPSC frequency of ACC neurons was significantly increased in mCCD group than that of sham group, while there is no significant difference in the amplitude of sEPSCs among them (Fig. 7a, b and f). Bath application of NS1619 (10 μM) caused a significant reduction in the sEPSC frequency of ACC neurons in mCCD rats (Fig. 7c, e and f). However, paxilline (10 μM) did not alter either the sEPSC frequency or amplitude of ACC neurons in sham rats (Fig. 7c, d and f). These findings indicate that the excitatory synaptic transmission of the ACC was enhanced and activation of BK_{Ca} channels with NS1619

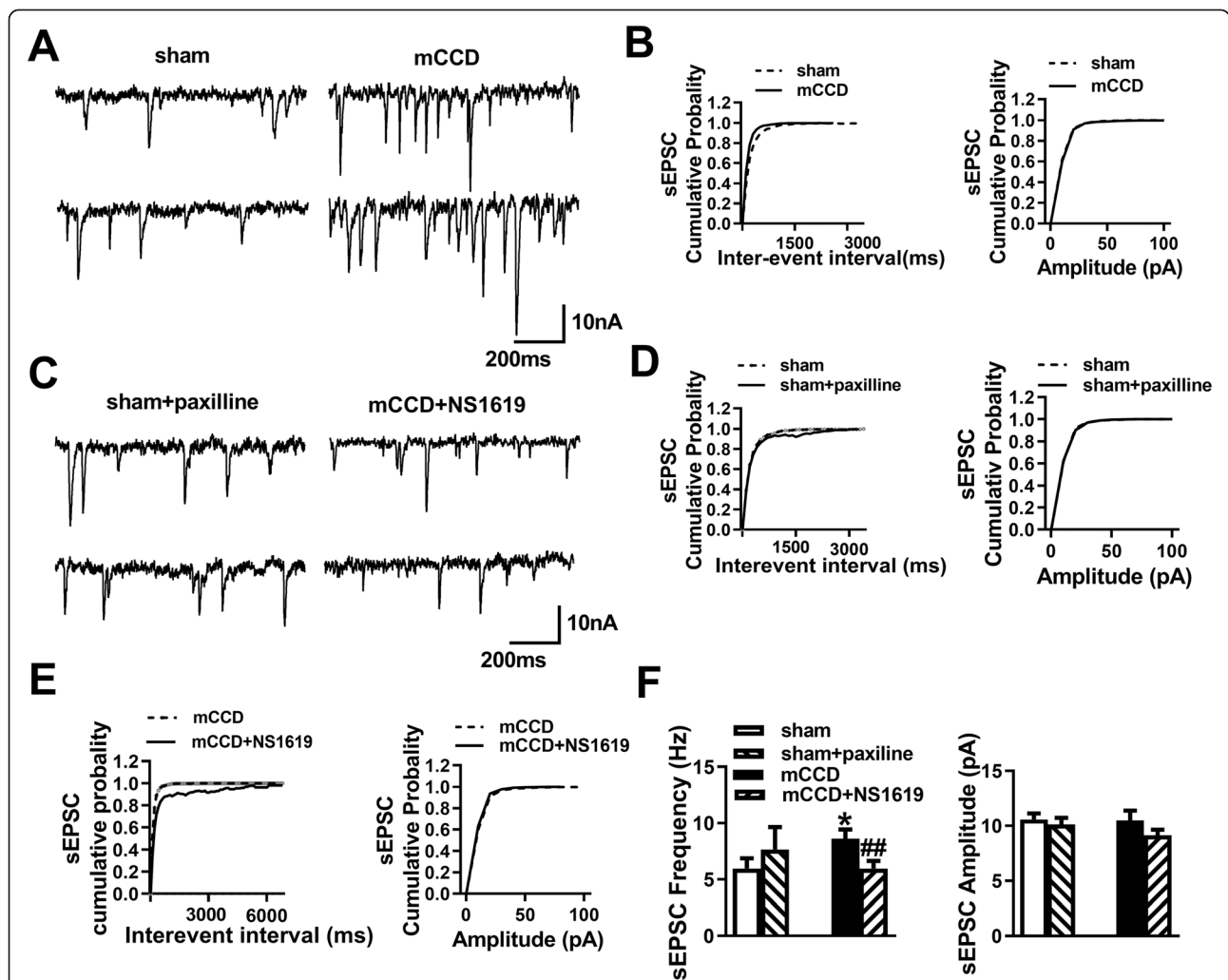


Fig. 7 NS1619 decreased the increased AMPA receptor-mediated sEPSC frequency of ACC neurons in mCCD rats. **a**, Representative sEPSCs recorded in ACC pyramidal neuron in slices from sham and mCCD rats at a holding potential of -60 mV; **b**, Cumulative interevent interval (top) and amplitude (bottom) histograms of sEPSCs; **c**, Representative traces show AMPA receptor-mediated sEPSCs in the presence of paxilline ($10 \mu\text{M}$) in sham rats and those in the presence of NS1619 ($10 \mu\text{M}$) in mCCD rats; **d**, Cumulative interevent interval and amplitude histograms of sEPSCs in the presence of paxilline ($10 \mu\text{M}$) in sham rats; **e**, Cumulative interevent interval and amplitude histograms of sEPSCs of ACC neurons in the presence of NS1619 in mCCD rats; **f**, Summary plots of sEPSC peak frequency and amplitude in the presence of paxilline ($10 \mu\text{M}$) in sham rats and those in the presence of NS1619 ($10 \mu\text{M}$) in mCCD rats ($n = 13$ neurons for sham and $n = 16$ neurons for mCCD). * $p < 0.05$, compared to the value of sham group, # $p < 0.05$, ## $p < 0.01$ compared with that of mCCD group

(10 μ M) induced a significant reduction in increased AMPAR-sEPSC frequencies of ACC neurons following mCCD.

NS1619 increased the paired-pulse ratios (PPR) of ACC neurons in mCCD rats

To validate our hypothesis, we further recorded the PPR of ACC neurons in mCCD rats. PPR is a transient form of plasticity used commonly as a measure of presynaptic function, in which the response to the second stimulus is enhanced as a result of residual calcium in the presynaptic terminal after the first stimulus [48, 49]. Our results showed that PPR at a stimulus interval of 50 ms was significantly reduced in ACC pyramidal neurons from mCCD rats and NS1619 can rescue this reduction (Fig. 8). However, paxilline did not alter the PPR of ACC neurons in sham rats. Together, these results indicate that the enhanced excitatory synaptic transmission is attributable to

an increase in the probability of presynaptic neurotransmitter release and BK_{Ca} channels are functionally linked to the synaptic transmission following nerve injury.

Local activation of BK_{Ca} channels in the ACC reversed neuropathic pain and anxiety-like behaviors

Our results showed that the function of the BK_{Ca} channels were down-regulated in the ACC after neuropathic pain. To test whether ACC BK_{Ca} channels may contribute to behavioral sensitization and anxiety-like behaviors in mCCD rats, we microinjected the BK_{Ca} channels opener NS1619 into the ACC and evaluated the effect of NS1619 on the pain threshold of the injured and contralateral feet and anxiety-like behaviors (Fig. 9a). Bilateral infusion with NS1619 (10 μ M, 0.5 μ l) reversed neuropathic pain associated anxiety-like behavior in EPM exploration, measured as time in the open arms, between NS1619 and ACSF injected animals (Fig. 9b). Similarly, in the open field test,

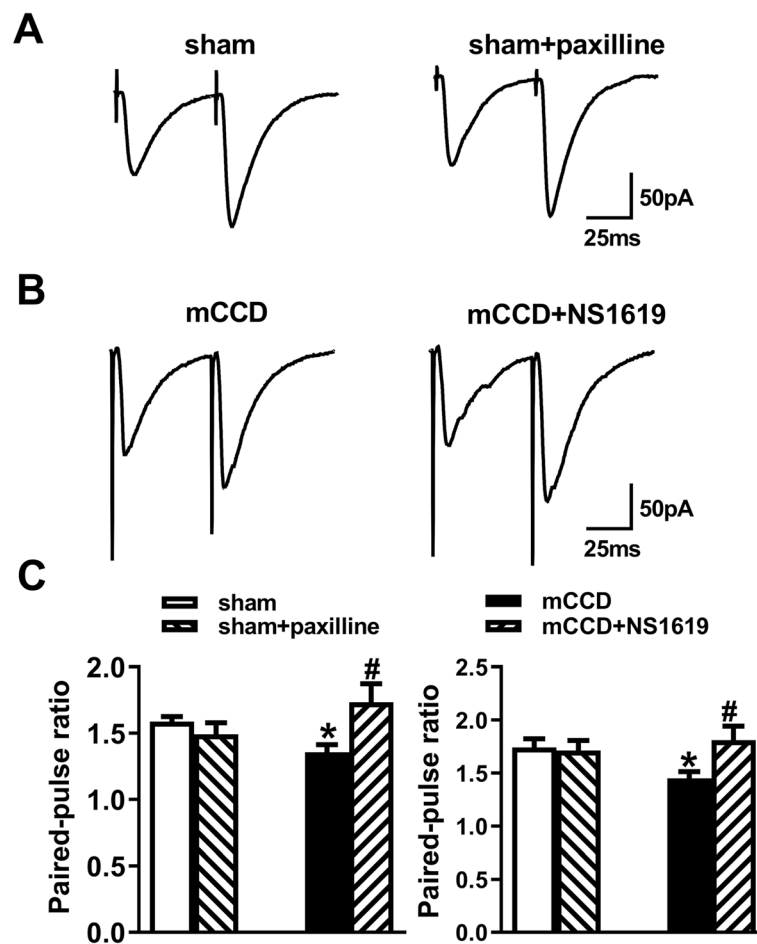


Fig. 8 NS1619 enhanced the decreased PPR of ACC neurons in mCCD rats. **a-b**, Representative traces with an interval of 50 ms recorded in layer II/III of the ACC; **a**, PPR (the ratio of EPSC2 / EPSC1) were recorded at intervals of 50 ms from sham rats (n = 6 neurons in the absence or presence of paxilline (10 μ M)). **b**, PPR were recorded at intervals of 50 ms from mCCD rats (n = 8 neurons in the absence or presence of NS1619 (10 μ M)). **c**, Summary plots of PPR at intervals of 50 ms from sham and mCCD rats (n = 6 neurons for sham and n = 8 neurons for mCCD), and effects of paxilline and NS1619 on PPR of sham and mCCD rats respectively. *p < 0.05 compared with that of sham group, #p < 0.05 compared to that of mCCD group

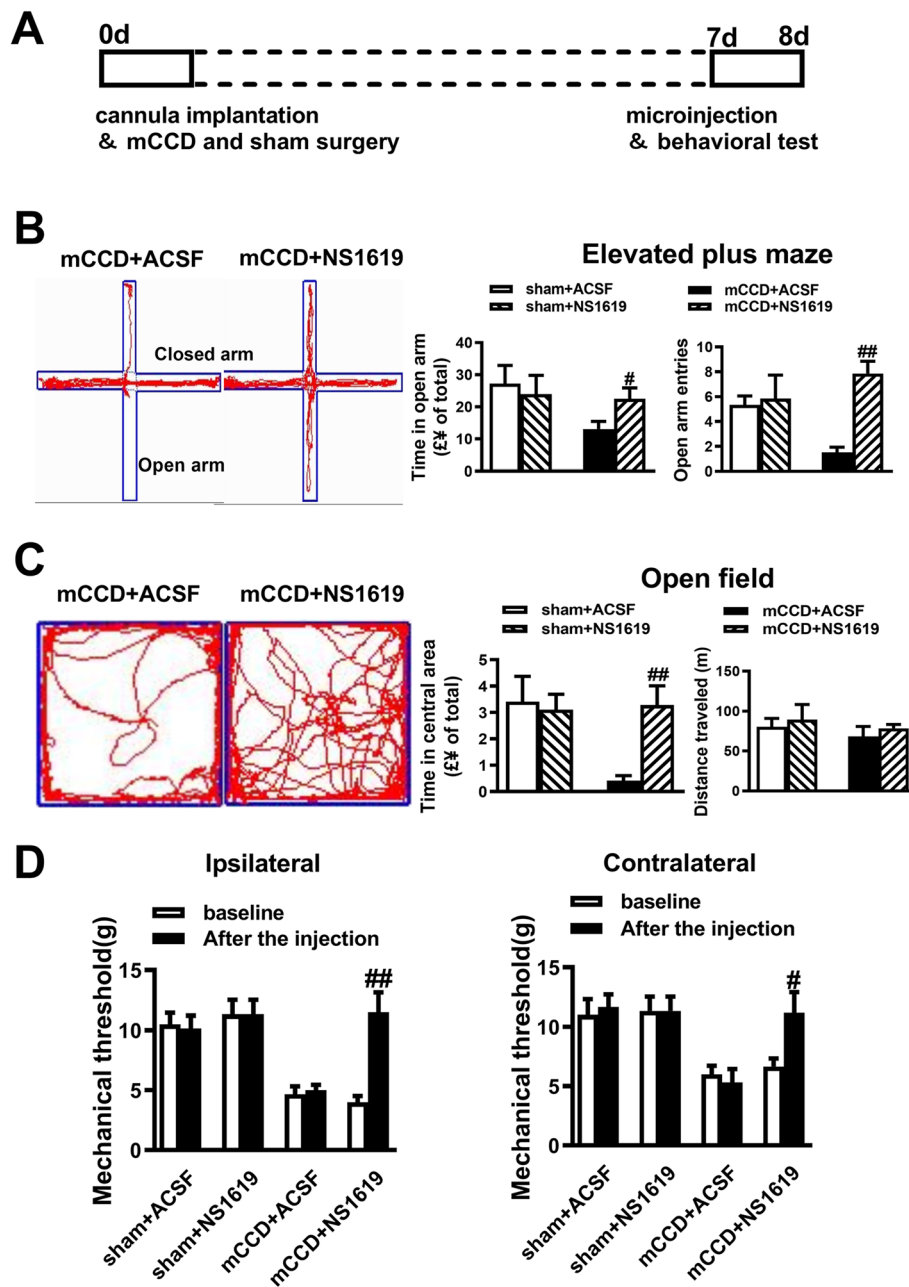


Fig. 9 Effects of activating BK_{Ca} channels in the ACC on neuropathic pain and anxiety-like behaviors. **a**, A schematic diagram of microinjection and the behavioral experiment. **b**, Bilateral microinjection of NS1619 (10 μM, 0.5 μL) into the ACC reversed the time in the open arms and the open arm entries in mCCD rats on day 7 after surgery. **c**, Rats infused with NS1619 spent more time in the central areas in open field test in mCCD rats compared with ACSF-treated animals. There was no significant difference in the total distance travelled within the open field for 15 min among mCCD and sham rats (sham + ACSF: n = 6, sham + NS1619: n = 6, mCCD + ACSF: n = 6, mCCD + NS1619: n = 6). **d**, The pain threshold of the injured hind paw (left) and contralateral feet (right), after bilateral microinjection of NS1619 into the ACC on day 7 after surgery. #*p* < 0.05, ##*p* < 0.01 compared with that of mCCD with ACSF group

mCCD rats spent more time in the central areas after treatment with NS1619 compared with those injected with ACSF (Fig. 9c). There was no significant difference in terms of the total distance travelled within the open field for 15mins, indicating that motor coordination and motor function were not changed in all rats examined (Fig. 9c).

After bilateral infusion of NS1619 into the ACC on post-surgical day 7, behavioral sensitization of both injured and contralateral hind paws were significantly reversed compared with those of saline microinjection (Fig. 9d). However, NS1619 did not alter the mechanical sensitivity in sham rats compared to a ACSF group (Fig. 9d). This

demonstrates that pharmacological activation of BK_{Ca} channels can reverse the effects of neuropathic pain.

Discussion

The present study provided the strong evidence that mCCD rats exhibited an enhanced anxiety-like behavior, which accompanied bilateral mechanical hypersensitivity. The upregulated expression of the auxiliary BK_{Ca} β4 subunit in the ACC induced the downregulated function of BK_{Ca} channels in the ACC following neuropathic pain. Presynaptic and postsynaptic upregulation of BKβ4 subunit may be involved in increased neuronal excitability and synaptic transmission in the ACC in neuropathic pain state. Local activation of BK_{Ca} channels in the ACC reversed neuropathic pain and anxiety-like behaviors. These results suggest that the upregulated expression of BK_{Ca} β4 subunit in the ACC might contribute to anxiety-like behaviors following neuropathic pain.

Upregulation of postsynaptic auxiliary BK_{Ca} β4 subunit in the ACC might contribute to anxiety-like behaviors following neuropathic pain

BK_{Ca} channels are known as large single-channel conductance of 100–300 pS among the super family of potassium channels, and dual activation by membrane depolarization and increases in intracellular calcium concentration [50–53]. BK_{Ca} channels play important roles in the regulation of action potentials and excitability in neurons, such as the repolarization of the AP as well as the fAHP [54–56]. Our results showed an enhanced anxiety-like behavior accompanied neuropathic pain in mCCD rats and an increase in the intrinsic excitability of ACC pyramidal neurons of mCCD rats including a decrease of fAHP, rheobase, and action potential amplitude and an increase of R_m, AP duration, half-width and decay time. The increased excitability in ACC neurons of mCCD rats was in line with that of ACC neurons following nerve ligation [40]. The changes of a decrease of fAHP, rheobase, and action potential amplitude and an increase of R_m, AP duration, half-width and decay time strongly indicate a reduction of function and/or expression in BK_{Ca} channels in ACC pyramidal neurons of mCCD rats. In the meantime, NS1619, an agonist of BK_{Ca} channels, significantly rescued the alteration of fAHP and AP duration in ACC pyramidal neurons in the mCCD rat. And paxilline, an inhibitor of BK_{Ca} channels, failed to influence the fAHP peak of ACC pyramidal neurons in the sham rat. All these data confirmed that down-regulated function of BK_{Ca} channels contributed to the alteration of AP repolarization and fAHP in ACC neurons in neuropathic pain state. Consistently, our results further showed that BK_{Ca}

current was markedly decreased in ACC neurons of the mCCD rat. These results were also similar to the decrease of BK_{Ca} currents in dorsal root ganglion neurons in neuropathic pain [30, 31, 57], and in CA3 pyramidal neuron of Fmr1 knock-out mice with anxiety-like behavior [58]. In contrast to the down regulation of alpha subunit of BK_{Ca} channels in the lateral amygdala (LA) [32], our molecular biological data showed the up-regulation of mRNA and protein expression of BK_{Ca} β4 subunit were specially increased in the ACC following mCCD. BK_{Ca} channels can be associated with accessory β subunits. Every β subunit has a specific tissue distribution and that they modify channel kinetics as well as their pharmacological properties and the apparent Ca²⁺ sensitivity of the α subunit in different ways [23]. Although previous studies showed that β4 increased BK_{Ca} channel to open [59, 60], β4 subunit could be regarded as an inhibitory neuronal subunit of BK_{Ca} channels [24, 61, 62]. Our results showed that BK currents were decreased in the ACC due to the up-regulation of BK_{Ca} β4 subunit following nerve injury. It is suggested the inhibitory effect of the up-regulation of β4 subunit on the function of BK_{Ca} channels in the ACC in neuropathic pain associated with anxiety-like behavior. In addition, our results further demonstrated that pharmacological enhancement of BK_{Ca} channel function in the ACC reversed neuropathic pain and anxiety-like behaviors. A previous study showed that the activation of BK_{Ca} channels in the LA reversed stress-induced anxiety-like behavior [32]. Recently, it was reported that a selective BK_{Ca} channel opener reversed impaired non-social anxiety-like behavior [63]. Previous studies showed the sensory component of chronic pain remains functionally segregated from its affective and anxiodepressive components at cortical level [1, 64]. However, our data showed the modulation of BK_{Ca} channels might share similar mechanisms in the ACC underlying anxiety-like behaviors accompanied with neuropathic pain.

Membrane-bound calcium-stimulated adenylyl cyclase1 (AC1) is specifically and highly expressed in cortical neurons including the ACC and the insular cortex [49, 65–67]. Recent studies suggest that the surface trafficking of BK_{Ca} channels can be modulated by signaling cascades and assembly with accessory proteins [68], and BK_{Ca} β4 surface trafficking must be post-transcriptionally regulated [69]. Moreover, BK_{Ca} β4 subunit is largely retained in intracellular compartments through an endoplasmic reticulum (ER) retention signal [70, 71]. More recently an imaging research demonstrated that activation of AC reduced BK_{Ca} α surface levels in HEK293 cells with fluorogen activating peptide [68]. These studies indicate that it is very likely that AC1 may modulate the trafficking of BK_{Ca} channels in the ACC in neuropathic pain.

Upregulation of presynaptic BK_{Ca} β4 subunit in synaptic transmission in the ACC in neuropathic pain state

Modulation of presynaptic AP duration exerts a precise and powerful mechanism to control and regulate neurotransmitter release. AP duration is a critical determinant for transmitter release, controlling the amount of presynaptic calcium influx, which translates electric changes to the release magnitude of neurotransmitters. The AP duration is controlled primarily by the activity of voltage-gated K⁺ channels (VGKCs) [72]. Among VGKCs, BK_{Ca} channels mainly determine AP duration during repetitive activity, owing to their activation being both voltage and calcium regulated in central neurons [55]. For example, BK_{Ca} channels control transmitter release in the synapse [47, 56, 73, 74]. FMRP regulates neurotransmitter release and short-term plasticity through presynaptic BK_{Ca} channels in hippocampal pyramidal neurons [58]. Our data showed that sEPSC frequency was significantly increased in the ACC in mCCD rats. Consistent with our previous results, neuropathic pain causes presynaptic enhancement of the excitatory synaptic transmission in the ACC [49]. And upregulation of presynaptic BK_{Ca} β4 subunit results in a slower repolarization of action potentials which in turn increase the amount of Ca²⁺ flowing into the cell in the ACC following neuropathic pain. Moreover, an agonist of BK_{Ca} channels decreased the increased AMPA receptor-mediated sEPSC frequency and increased the decreased PPR of ACC neurons of mCCD rats. Activation of BK_{Ca} channel function in the ACC reversed neuropathic pain and anxiety-like behaviors.

Taken together, these results indicate that the upregulation of presynaptic BK_{Ca} β4 subunit might also increase basic synaptic transmission in a presynaptic modulation. BK_{Ca} channels mediated neuropathic pain induced anxiety-like behaviors via the increase of presynaptic neurotransmitter release.

Conclusions

In summary, our study indicated presynaptic and postsynaptic up-regulation of BK_{Ca} β4 subunit in neuronal excitability and synaptic transmission in the ACC in neuropathic pain state. In physiological states, BK_{Ca} β4 subunit is expressed in both presynaptic and postsynaptic neurons, the opening of BK_{Ca} channels allows rapid efflux of potassium ions, which effectively hyperpolarizes membrane potential. In neuropathic pain states, the upregulation of postsynaptic BK_{Ca} β4 subunit induces neuronal activation easily due to the loss function of BK_{Ca} channels. In the meantime, the upregulation of presynaptic BK_{Ca} β4 subunit results in a more slow repolarization of action potentials which in turn increases the amount of Ca²⁺ flowing into the cell. Thus BK_{Ca} channels enhance the transmitter release in the synapse in the ACC in neuropathic pain state. All these data

provided evidence that BK_{Ca} pathway has to be explored as a new interesting therapeutic target for neuropathic pain-associated anxiety. Therefore, our results suggested that BK_{Ca} channel agonist might be a potential candidate for pain-related anxiety treatment because it suppresses neuronal hyperexcitability and decreases neurotransmitter release at the synapse in the ACC following neuropathic pain.

Acknowledgements

We appreciate the support from the National Natural Science Foundation of China(81671081 and 31371120 to Dr. H.X.) and University Science & Technology Fund Planning Project (2019XB006 to Dr. H.X.). Also thank Drs. Minggao Zhao and Tao Chen for their helpful comments on the manuscript.

Authors' contributions

Conceived and designed the experiments: HX and HZ. Performed the experiments: HZ, QX, CL, SH, QW, YZ, TY, YX, HF, CL, FM, MZ. Analyzed the data: HZ, CL and QX. Provided technical platform support: YZ, XW and SW. Wrote the paper: HX, HZ, MZ. All authors read and approved the final manuscript.

Funding

This work was supported by the National Natural Science Foundation of China(81671081 and 31371120 to Dr. H.X.) and University Science & Technology Fund Planning Project (2019XB006 to Dr. H.X.)

Availability of data and materials

On behalf of all authors, we declare that the data and material in the manuscript are original and the manuscript is not under consideration for publication elsewhere. In addition, none of the manuscript contents has been previously published.

Ethics approval and consent to participate

All experimental protocols were approved by the Institutional Animal Care and Use Committee of FMMU and animals were maintained and cared for in line with the guidelines set forth by the International Association for the Study of Pain.

Consent for publication

Not applicable.

Competing interests

The authors declare that they have no competing interests.

Author details

¹Department of Neurobiology and Collaborative Innovation Center for Brain Science, School of Basic Medicine, Fourth Military Medical University, Xi'an 710032, China. ²Center for Neuron and Disease, Frontier Institute of Science and Technology, Xi'an Jiaotong University, Xi'an 710049, China. ³Department of Physiology, University of Toronto, Toronto, Canada. ⁴Department of Anesthesiology, Heze Municipal Hospital, Heze 274031, Shandong, China. ⁵Shandong First Medical University & Shandong Academy of Medical Sciences, Taian 271000, Shandong, China. ⁶Key Laboratory for Space Bioscience and Biotechnology, School of Life Sciences, Northwestern Polytechnical University, Xi'an 710072, China. ⁷Department of Burns and Cutaneous Surgery, Xijing Hospital, Fourth Military Medical University, Xi'an 710032, China.

Received: 16 December 2019 Accepted: 19 January 2020

Published online: 18 February 2020

References

- Barthas F, Sellmeijer J, Hugel S, Waltisperger E, Barrot M, Yalcin I. The anterior cingulate cortex is a critical hub for pain-induced depression. *Biol Psychiatry*. 2015;77(3):236–45.
- Bliss TV, Collingridge GL, Kaang BK, Zhuo M. Synaptic plasticity in the anterior cingulate cortex in acute and chronic pain. *Nat Rev Neurosci*. 2016; 17(8):485–96.

3. Zhuo M. Cortical excitation and chronic pain. *Trends Neurosci.* 2008;31(4):199–207.
4. Zhuo M. Neural mechanisms underlying anxiety-chronic pain interactions. *Trends Neurosci.* 2016;39(3):136–45.
5. Sun YG, Gao YJ, Zhao ZQ, Huang B, Yin J, Taylor GA, Chen ZF. Involvement of P311 in the affective, but not in the sensory component of pain. *Molecular pain.* 2008;4:23.
6. Lueboonthavatchai P. Prevalence and psychosocial factors of anxiety and depression in breast cancer patients. *J Med Assoc Thai.* 2007;90(10):2164–74.
7. Narita M, Kaneko C, Miyoshi K, Nagumo Y, Kuzumaki N, Nakajima M, Nanjo K, Matsuzawa K, Yamazaki M, Suzuki T. Chronic pain induces anxiety with concomitant changes in opioidergic function in the amygdala. *Neuropsychopharmacology.* 2006;31(4):739–50.
8. Sieberg CB, Taras C, Gomaa A, Nickerson C, Wong C, Ward C, Baskozos G, Bennett DLH, Ramirez JD, Themistocleous AC, Rice ASC, Shillo PR, Tesfaye S, Edwards RR, Andrews NA, Berde C, Costigan M. Neuropathic pain drives anxiety behavior in mice, results consistent with anxiety levels in diabetic neuropathy patients. *Pain reports.* 2018;3(3):e651.
9. Wang GQ, Cen C, Li C, Cao S, Wang N, Zhou Z, Liu XM, Xu Y, Tian NX, Zhang Y, Wang J, Wang LP, Wang Y. Deactivation of excitatory neurons in the prefrontal cortex via Cdk5 promotes pain sensation and anxiety. *Nature Communications.* 2015;6:7660.
10. Bair MJ, Brizendine EJ, Ackermann RT, Shen C, Kroenke K, Marrero DG. Prevalence of pain and association with quality of life, depression and glycaemic control in patients with diabetes. *Diabetic Med.* 2010;27(5):578–84.
11. Gore M, Brandenburg NA, Dukes E, Hoffman DL, Tai KS, Stacey B. Pain severity in diabetic peripheral neuropathy is associated with patient functioning, symptom levels of anxiety and depression, and sleep. *J Pain Symptom Manag.* 2005;30(4):374–85.
12. Baptista-de-Souza, D, Nunciato, AC, Pereira, BC, Fachinni, G, Zaniboni, CR & Canto-de-Souza, A. Mice undergoing neuropathic pain induce angiogenic-like effects and hypernociception in cagemates. *Behavioural pharmacology* 2015;26(7 Spec No): 664–672.
13. McCracken LM, Gross RT, Sorg PJ, Edmonds TA. Prediction of pain in patients with chronic low back pain: effects of inaccurate prediction and pain-related anxiety. *Behav Res Ther.* 1993;31(7):647–52.
14. Lerman SF, Rudich Z, Brill S, Shalev H, Shahar G. Longitudinal associations between depression, anxiety, pain, and pain-related disability in chronic pain patients. *Psychosom Med.* 2015;77(3):333–41.
15. Weisenberg M, Aviram O, Wolf Y, Raphaeli N. Relevant and irrelevant anxiety in the reaction to pain. *Pain.* 1984;20(4):371–83.
16. Rhudy JL, Meagher MW. Fear and anxiety: divergent effects on human pain thresholds. *Pain.* 2000;84(1):65–75.
17. Rivat C, Becker C, Blugeot A, Zeau B, Mauborgne A, Pohl M, Benoliel JJ. Chronic stress induces transient spinal neuroinflammation, triggering sensory hypersensitivity and long-lasting anxiety-induced hyperalgesia. *Pain.* 2010;150(2):358–68.
18. Kaufmann WA, Kasugai Y, Ferraguti F, Storm JF. Two distinct pools of large-conductance calcium-activated potassium channels in the somatic plasma membrane of central principal neurons. *Neuroscience.* 2010;169(3):974–86.
19. Piwońska M, Wilczek E, Szewczyk A, Wilczynski GM. Differential distribution of Ca²⁺-activated potassium channel beta4 subunit in rat brain: immunolocalization in neuronal mitochondria. *Neuroscience.* 2008;153(2):446–60.
20. Farajnia S, Meijer JH, Michel S. Age-related changes in large-conductance calcium-activated potassium channels in mammalian circadian clock neurons. *Neurobiol Aging.* 2015;36(6):2176–83.
21. Rohmann KN, Wersinger E, Braude JP, Pyott SJ, Fuchs PA. Activation of BK and SK channels by efferent synapses on outer hair cells in high-frequency regions of the rodent cochlea. *J Neurosci.* 2015;35(5):1821–30.
22. Sachse G, Faulhaber J, Seniuk A, Ehmke H, Pongs O. Smooth muscle BK channel activity influences blood pressure independent of vascular tone in mice. *J Physiol.* 2014;592(12):2563–74.
23. Torres YP, Granados ST, Latorre R. Pharmacological consequences of the coexpression of BK channel alpha and auxiliary beta subunits. *Frontiers in physiology.* 2014;5:383.
24. Behrens R, Nolting A, Reimann F, Schwarz M, Waldschutz R, Pongs O. hKCNMB3 and hKCNMB4, cloning and characterization of two members of the large-conductance calcium-activated potassium channel beta subunit family. *FEBS Lett.* 2000;474(1):99–106.
25. Tian L, Coghill LS, McClafferty H, MacDonald SH, Antoni FA, Ruth P, Knaus HG, Shipston MJ. Distinct stoichiometry of BK_{Ca} channel tetramer phosphorylation specifies channel activation and inhibition by cAMP-dependent protein kinase. *Proc Natl Acad Sci U S A.* 2004;101(32):11897–902.
26. Yan J, Aldrich RW. LRRC26 auxiliary protein allows BK channel activation at resting voltage without calcium. *Nature.* 2010;466(7305):513–6.
27. Yan J, Olsen JV, Park KS, Li W, Bildl W, Schulte U, Aldrich RW, Fakler B, Trimmer JS. Profiling the phospho-status of the BK_{Ca} channel alpha subunit in rat brain reveals unexpected patterns and complexity. *Molecular & cellular proteomics : MCP.* 2008;7(11):2188–98.
28. Jaffe DB, Wang B, Brenner R. Shaping of action potentials by type I and type II large-conductance Ca²⁺-activated K⁺ channels. *Neuroscience.* 2011;192:205–18.
29. Muller A, Kukley M, Uebachs M, Beck H, Dietrich D. Nanodomains of single Ca²⁺ channels contribute to action potential repolarization in cortical neurons. *J Neurosci.* 2007;27(3):483–95.
30. Cao XH, Chen SR, Li L, Pan HL. Nerve injury increases brain-derived neurotrophic factor levels to suppress BK channel activity in primary sensory neurons. *J Neurochem.* 2012;121(6):944–53.
31. Chen SR, Cai YQ, Pan HL. Plasticity and emerging role of BK_{Ca} channels in nociceptive control in neuropathic pain. *J Neurochem.* 2009;110(1):352–62.
32. Guo YY, Liu SB, Cui GB, Ma L, Feng B, Xing JH, Yang Q, Li XQ, Wu YM, Xiong LZ, Zhang W, Zhao MG. Acute stress induces down-regulation of large-conductance Ca²⁺-activated potassium channels in the lateral amygdala. *J Physiol.* 2012;590(4):875–86.
33. Xie YB, Zhao H, Wang Y, Song K, Zhang M, Meng FC, Yang YJ, He YS, Kuang F, You SW, You HJ, Xu H. Bilateral Neuropathy of Primary Sensory Neurons by the Chronic Compression of Multiple Unilateral DRGs. *Neural plasticity.* 2016;2016:2130901.
34. Chaplan SR, Bach FW, Pogrel JW, Chung JM, Yaksh TL. Quantitative assessment of tactile allodynia in the rat paw. *J Neurosci Methods.* 1994;53(1):55–63.
35. Novier A, Van Skike CE, Diaz-Granados JL, Mittleman G, Matthews DB. Acute alcohol produces ataxia and cognitive impairments in aged animals: a comparison between young adult and aged rats. *Alcohol Clin Exp Res.* 2013;37(8):1317–24.
36. Rustay NR, Wahlsten D, Crabbe JC. Influence of task parameters on rotarod performance and sensitivity to ethanol in mice. *Behav Brain Res.* 2003;141(2):237–49.
37. Pacchioni AM, Kalivas PW. The role of AMPAR trafficking mediated by neuronal Pentraxins in cocaine-induced Neuroadaptations. *Mol Cell Pharmacol.* 2009;1(2):183–92.
38. Milnerwood AJ, Gladding CM, Pouladi MA, Kaufman AM, Hines RM, Boyd JD, Ko RW, Vasuta OC, Graham RK, Hayden MR, Murphy TH, Raymond LA. Early increase in extrasynaptic NMDA receptor signaling and expression contributes to phenotypic onset in Huntington's disease mice. *Neuron.* 2010;65(2):178–90.
39. Qiu S, Zhang M, Liu Y, Guo Y, Zhao H, Song Q, Zhao M, Haganir RL, Luo J, Xu H, Zhuo M. GluA1 phosphorylation contributes to postsynaptic amplification of neuropathic pain in the insular cortex. *J Neurosci.* 2014;34(40):13505–15.
40. Cao XY, Xu H, Wu LJ, Li XY, Chen T, Zhuo M. Characterization of intrinsic properties of cingulate pyramidal neurons in adult mice after nerve injury. *Molecular Pain.* 2009;5:73.
41. Neely A, Lingle CJ. Two components of calcium-activated potassium current in rat adrenal chromaffin cells. *The Journal of physiology.* 1992;453:97–131.
42. Goodman MB, Art JJ. Variations in the ensemble of potassium currents underlying resonance in turtle hair cells. *The Journal of physiology.* 1996;497(Pt 2):395–412.
43. Li W, Gao SB, Lv CX, Wu Y, Guo ZH, Ding JP, Xu T. Characterization of voltage- and Ca²⁺-activated K⁺ channels in rat dorsal root ganglion neurons. *J Cell Physiol.* 2007;212(2):348–57.
44. Imlach WL, Finch SC, Zhang Y, Dunlop J, Dalziel JE. Mechanism of action of lolitrem B, a fungal endophyte derived toxin that inhibits BK large conductance Ca²⁺-activated K⁺ channels. *Toxicol.* 2011;57(5):686–94.
45. Sanchez M, McManus OB. Paxilline inhibition of the alpha-subunit of the high-conductance calcium-activated potassium channel. *Neuropharmacology.* 1996;35(7):963–8.
46. Holmes PV. Rodent models of depression: reexamining validity without anthropomorphic inference. *Crit Rev Neurobiol.* 2003;15(2):143–74.
47. Raffaelli G, Saviane C, Mohajerani MH, Pedarzani P, Cherubini E. BK potassium channels control transmitter release at CA3-CA3 synapses in the rat hippocampus. *J Physiol.* 2004;557(Pt 1):147–57.
48. Foster TC, McNaughton BL. Long-term enhancement of CA1 synaptic transmission is due to increased quantal size, not quantal content. *Hippocampus.* 1991;1(1):79–91.
49. Xu H, Wu LJ, Wang H, Zhang X, Vadakkan KI, Kim SS, Steenland HW, Zhuo M. Presynaptic and postsynaptic amplifications of neuropathic pain in the anterior cingulate cortex. *J Neurosci.* 2008;28(29):7445–53.
50. Golowasch J, Kirkwood A, Miller C. Allosteric effects of Mg²⁺ on the gating of Ca²⁺-activated K⁺ channels from mammalian skeletal muscle. *The Journal of experimental biology.* 1986;124:5–13.

51. Latorre R, Miller C. Conduction and selectivity in potassium channels. *J Membr Biol.* 1983;71(1–2):11–30.
52. Latorre R, Oberhauser A, Labarca P, Alvarez O. Varieties of calcium-activated potassium channels. Annual review of physiology. 1989;51:385–99.
53. Marty A. Ca-dependent K channels with large unitary conductance in chromaffin cell membranes. *Nature.* 1981;291(5815):497–500.
54. Dopico AM, Bukiya AN, Martin GE. Ethanol modulation of mammalian BK channels in excitable tissues: molecular targets and their possible contribution to alcohol-induced altered behavior. *Frontiers in physiology.* 2014;5:466.
55. Salkoff L, Butler A, Ferreira G, Santi C, Wei A. High-conductance potassium channels of the SLO family. *Nat Rev Neurosci.* 2006;7(12):921–31.
56. Samengo I, Curro D, Barrese V, Tagliatalata M, Martire M. Large conductance calcium-activated potassium channels: their expression and modulation of glutamate release from nerve terminals isolated from rat trigeminal caudal nucleus and cerebral cortex. *Neurochem Res.* 2014;39(5):901–10.
57. Liu CY, Lu ZY, Li N, Yu LH, Zhao YF, Ma B. The role of large-conductance, calcium-activated potassium channels in a rat model of trigeminal neuropathic pain. *Cephalgia.* 2015;35(1):16–35.
58. Deng PY, Rotman Z, Blundon JA, Cho Y, Cui J, Cavalli V, Zakharenko SS, Klyachko VA. FMRP regulates neurotransmitter release and synaptic information transmission by modulating action potential duration via BK channels. *Neuron.* 2013;77(4):696–711.
59. Contreras GF, Neely A, Alvarez O, Gonzalez C, Latorre R. Modulation of BK channel voltage gating by different auxiliary beta subunits. *Proc Natl Acad Sci U S A.* 2012;109(46):18991–6.
60. Wang B, Rothberg BS, Brenner R. Mechanism of beta4 subunit modulation of BK channels. *The Journal of general physiology.* 2006;127(4):449–65.
61. Brenner R, Chen QH, Vilaythong A, Toney GM, Noebels JL, Aldrich RW. BK channel beta4 subunit reduces dentate gyrus excitability and protects against temporal lobe seizures. *Nat Neurosci.* 2005;8(12):1752–9.
62. Weiger TM, Holmqvist MH, Levitan IB, Clark FT, Sprague S, Huang WJ, Ge P, Wang C, Lawson D, Jurman ME, Glucksmann MA, Silos-Santiago I, DiStefano PS, Curtis R. A novel nervous system beta subunit that downregulates human large conductance calcium-dependent potassium channels. *J Neurosci.* 2000;20(10):3563–70.
63. Hebert B, Pietropaolo S, Meme S, Laudier B, Laugeray A, Doisne N, Quartier A, Lefeuvre S, Got L, Cahard D, Laumonier F, Crusio WE, Pichon J, Menuet A, Perche O, Briault S. Rescue of fragile X syndrome phenotypes in Fmr1 KO mice by a BK_{Ca} channel opener molecule. *Orphanet journal of rare diseases.* 2014;9:124.
64. Koga K, Descalzi G, Chen T, Ko HG, Lu J, Li S, Son J, Kim T, Kwak C, Haganir RL, Zhao MG, Kaang BK, Collingridge GL, Zhuo M. Coexistence of two forms of LTP in ACC provides a synaptic mechanism for the interactions between anxiety and chronic pain. *Neuron.* 2015;85(2):377–89.
65. Vadakkan KI, Wang H, Ko SW, Zastepa E, Petrovic MJ, Sluka KA, Zhuo M. Genetic reduction of chronic muscle pain in mice lacking calcium/calmodulin-stimulated adenylyl cyclases. *Mol Pain.* 2006;2:7.
66. Wang H, Xu H, Wu LJ, Kim SS, Chen T, Koga K, Descalzi G, Gong B, Vadakkan KI, Zhang X, Kaang BK, Zhuo M. Identification of an adenylyl cyclase inhibitor for treating neuropathic and inflammatory pain. *Science translational medicine.* 2011;3(65):65ra63.
67. Wei F, Qiu CS, Kim SJ, Muglia L, Maas JW, Pineda VV, Xu HM, Chen ZF, Storm DR, Muglia LJ, Zhuo M. Genetic elimination of behavioral sensitization in mice lacking calmodulin-stimulated adenylyl cyclases. *Neuron.* 2002;36(4):713–26.
68. Pratt CP, He J, Wang Y, Barth AL, Bruchez MP. Fluorogenic green-inside red-outside (GIRO) labeling approach reveals adenylyl Cyclase-dependent control of BK α surface expression. *Bioconjug Chem.* 2015;26(9):1963–71.
69. Wang B, Jaffe DB, Brenner R. Current understanding of iberiotoxin-resistant BK channels in the nervous system. *Frontiers in physiology.* 2014;5:382.
70. Cox N, Toro B, Pacheco-Otalora LF, Garrido-Sanabria ER, Zarei MM. An endoplasmic reticulum trafficking signal regulates surface expression of beta4 subunit of a voltage- and Ca²⁺(+)-activated K(+) channel. *Brain Research.* 2014;1553:12–23.
71. Shruti S, Urban-Ciecko J, Fitzpatrick JA, Brenner R, Bruchez MP, Barth AL. The brain-specific Beta4 subunit downregulates BK channel cell surface expression. *PLoS One.* 2012;7(3):e33429.
72. Martina M, Metz AE, Bean BP. Voltage-dependent potassium currents during fast spikes of rat cerebellar Purkinje neurons: inhibition by BDS-I toxin. *J Neurophysiol.* 2007;97(1):563–71.
73. Roberts WM, Jacobs RA, Hudspeth AJ. Colocalization of ion channels involved in frequency selectivity and synaptic transmission at presynaptic active zones of hair cells. *J Neurosci.* 1990;10(11):3664–84.
74. Robitaille R, Garcia ML, Kaczorowski GJ, Charlton MP. Functional colocalization of calcium and calcium-gated potassium channels in control of transmitter release. *Neuron.* 1993;11(4):645–55.

Publisher's Note

Springer Nature remains neutral with regard to jurisdictional claims in published maps and institutional affiliations.

Ready to submit your research? Choose BMC and benefit from:

- fast, convenient online submission
- thorough peer review by experienced researchers in your field
- rapid publication on acceptance
- support for research data, including large and complex data types
- gold Open Access which fosters wider collaboration and increased citations
- maximum visibility for your research: over 100M website views per year

At BMC, research is always in progress.

Learn more biomedcentral.com/submissions

